A cold phase of the East Pacific triggers new phytoplankton blooms in San Francisco Bay

James E. Cloern*[†], Alan D. Jassby[‡], Janet K. Thompson*, and Kathryn A. Hieb[§]

*United States Geological Survey, MS496, 345 Middlefield Road, Menlo Park, CA 94025; [‡]Department of Environmental Science and Policy, University of California, Davis, CA 95616; and [§]California Department of Fish and Game, 4001 North Wilson Way, Stockton, CA 95205

Ecological observations sustained over decades often reveal abrupt changes in biological communities that signal altered ecosystem states. We report a large shift in the biological communities of San Francisco Bay, first detected as increasing phytoplankton biomass and occurrences of new seasonal blooms that began in 1999. This phytoplankton increase is paradoxical because it occurred in an era of decreasing wastewater nutrient inputs and reduced nitrogen and phosphorus concentrations, contrary to the guiding paradigm that algal biomass in estuaries increases in proportion to nutrient inputs from their watersheds. Coincidental changes included sharp declines in the abundance of bivalve mollusks, the key phytoplankton consumers in this estuary, and record high abundances of several bivalve predators: Bay shrimp, English sole, and Dungeness crab. The phytoplankton increase is consistent with a trophic cascade resulting from heightened predation on bivalves and suppression of their filtration control on phytoplankton growth. These community changes in San Francisco Bay across three trophic levels followed a state change in the California Current System characterized by increased upwelling intensity, amplified primary production, and strengthened southerly flows. These diagnostic features of the East Pacific ''cold phase'' lead to strong recruitment and immigration of juvenile flatfish and crustaceans into estuaries where they feed and develop. This study, built from three decades of observation, reveals a previously unrecognized mechanism of ocean–estuary connectivity. Interdecadal oceanic regime changes can propagate into estuaries, altering their community structure and efficiency of transforming land-derived nutrients into algal biomass.

climate variability | coastal eutrophication | ocean–estuary connectivity | regime shift | trophic cascade

E cosystem observations sustained over decades often produce surprises, revealing novel processes that regulate abundance, composition, and productivity of biological communities. In 1999, we were surprised by an October phytoplankton bloom in San Francisco Bay (SFB), a departure from the seasonal pattern observed over two preceding decades. This event signaled a large biological change manifesting over subsequent years as increasing phytoplankton biomass and new seasonal blooms. This change is puzzling because it occurred in an era of decreasing nutrient inputs. Phytoplankton increase is a well documented response to nutrient enrichment from fertilizer runoff and wastewater discharge to coastal ecosystems (1). Nutrient enrichment has promoted excessive algal production and severely degraded habitat quality in the Chesapeake Bay, northern Gulf of Mexico, and Baltic and Adriatic seas. The SFB "paradox" presented here is contrary to these experiences elsewhere and provides strong evidence that additional processes, beyond nutrient supply, can cause sustained increases in algal biomass. We use data from the United States Geological Survey (USGS) long-term study of SFB to describe the patterns of phytoplankton increase and then present evidence from other studies that the underlying process is a trophic cascade having origins in the Pacific Ocean.

Long-term research has been sustained in SFB, which exemplifies a large ecosystem at the land–sea interface influenced by natural processes of variability and multiple modes of human disturbance (2). SFB receives large inputs of nitrogen and phosphorus from its 153,000-km^2 agricultural watershed and its densely populated urban watershed. Nutrient inputs are comparable to those delivered to Chesapeake Bay, but SFB is a low-productivity estuary with no recurrent problems of hypoxia or harmful algal blooms (1). This eutrophication resistance has manifested over 20 years of observation as persistent low phytoplankton biomass and high nutrient concentrations. Median summer–autumn concentrations of dissolved inorganic nitrogen and phosphorus were 32.3 and 2.3 μM, respectively, in South SFB over the period 1977–1998. These values are 10 times higher than nutrient concentrations that limit phytoplankton growth, and they represent large stocks of unutilized nitrogen and phosphorus. Resistance mechanisms include tidal- and wind-driven mixing that prevent stratification, large sediment inputs and high turbidity that limits light penetration and phytoplankton photosynthesis, and fast filtration removal of phytoplankton cells by bivalve mollusks (3). Here, we report recent phytoplankton increases that signal a weakened resistance to nutrient pollution, and propose a top-down mechanism induced by a state change in the northeast Pacific Ocean. This study reveals how the expression of eutrophication from land runoff to estuaries can fluctuate with ocean-derived changes in biological community structure, a previously unrecognized mechanism of ocean–estuary connectivity with implications for how we study and manage nearshore coastal ecosystems.

Results

We have measured phytoplankton biomass as chlorophyll a (Chl-a) concentration at least monthly in SFB since 1978. Observations from 1978–1998 showed a recurrent annual pattern of low phytoplankton biomass punctuated by short-lived spring blooms. This pattern changed abruptly in 1999 with the first record of an autumn bloom, detected as elevated Chl-a at concentrations never observed during autumn sampling the previous 22 years (Fig. 1A). Autumn–winter blooms in subsequent years included unprecedented occurrences of dinoflagellate red tides (4). New seasonal blooms, coupled with increasing baseline Chl-a, have led to increased overall phytoplankton biomass (Fig. 1B). Trends over time (Theil–Sen slopes of decadal Chl-a series) revealed statistically significant ($P < 0.05$) phytoplankton increases beginning after 1999 (Fig. 1C). These changes

ECOLOGY

Fig. 1. Indicators of phytoplankton change in South SFB. (*A*) Occurrences of autumn blooms (August through December Chl-*a* >10) since 1999. (*B*) Increases in August through December Chl-*a* (interquartile ranges are shown as bars) and gross primary production (GPP) (open circles). (*C*) Ten-year windowed trends showing statistically significant (*P* < 0.05; filled squares) Chl-*a* increases after 1999. (*D*) Annual inputs of dissolved inorganic nitrogen and phosphorus from the San Jose–Santa Clara Wastewater Treatment Plant [N. Van Keuren (City of San Jose), personal communication], the largest municipal discharger to South SFB.

are also ecologically significant: estimated August through December primary production [supporting information (SI) *Text*] more than doubled (Fig. 1*B*), from 32 g C m^{-2} (pre-1998 mean) to 73 g C m^{-2} (post-1998 mean). Seasonal analysis of the 1978–2005 series detected positive Chl-*a* trends every month, of

which eight were statistically significant (Fig. 2*E*). These observations are compelling evidence of phytoplankton increase at a magnitude observed in other estuaries as a response to increasing nutrient input.

Water quality and biological communities of estuaries are strongly influenced by freshwater inputs that deliver sediments, nutrients, and contaminants from land runoff and wastewater discharge. South SFB is situated in a densely populated urban wat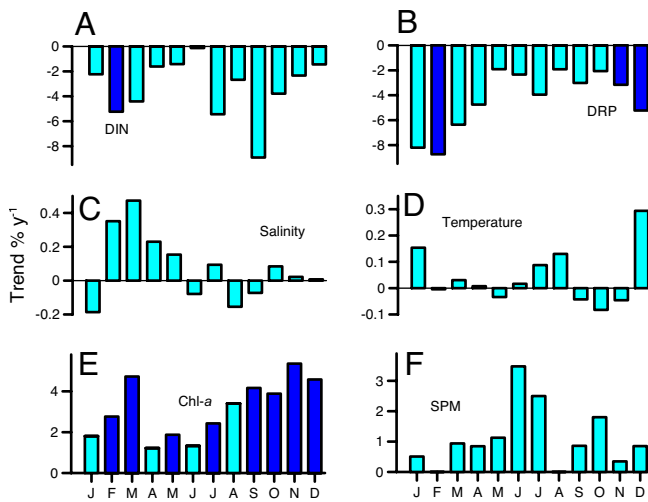ershed, and 98% of its nitrogen input (see table 8 of ref. 5) is from municipal wastewater treatment plants (North SFB is more strongly influenced by agricultural inputs from the Sacramento and San Joaquin rivers). We explored water-quality data for indicators that the phytoplankton increase in SFB was caused by changing inputs from the surrounding landscape that could increase algal growth rate. Phytoplankton biomass grows as algal cells divide at rates regulated by macronutrient (nitrogen, phosphorus) concentrations, water temperature, and light energy. But monthly trends of dissolved inorganic nitrogen (DIN) and dissolved reactive phosphorus (DRP) concentrations in SFB were negative for each month, approaching maximum trends of −10% y^{-1} (Fig. 2 *A* and *B*). These large nutrient declines are consistent with progressive improvements in municipal wastewater treatment leading to decreasing N and P input from the urban watershed (Fig. 1*D*) and expectations of a corresponding reduction in algal biomass.

Monthly trends of water temperature in SFB over the period 1978–2005 were small and not statistically significant (Fig. 2*D*). SFB has high concentrations of suspended sediments that limit light penetration and photosynthesis, a primary factor in this estuary's low productivity and low nutrient assimilation efficiency (1). But monthly trends of suspended particulate matter (SPM) were positive for each month (Fig. 2*F*), so turbidity and light limitation have not diminished over time. Algal blooms can be triggered by salinity stratification that creates a shallow high-light surface layer of fast phytoplankton growth (3). Salinity stratification of estuaries is strongest during years of high river flow and low surface salinity. Trends of surface salinity in SFB varied across months, but none were statistically significant (Fig. 2*C*), and there were no significant trends of stratification intensity (difference between bottom and surface salinity). We conclude that the phytoplankton increase in SFB was not caused by secular increases in the phytoplankton growth rate because nutrients have declined, turbidity has (weakly) increased, stratification has not strengthened, and water temperature has not changed inside the estuary.

We next explored biological monitoring data to consider an alternative, top-down explanation for the phytoplankton increase in SFB as a result of reduced consumption by herbivores. A large fraction of phytoplankton primary production in SFB is consumed by bivalve mollusks, and high bivalve biomass and filtration rates are keys to the low phytoplankton–high nutrient state. Summer–autumn rates of phytoplankton growth and bivalve consumption have historically been balanced (3), and simulations with a numerical model demonstrate a high sensitivity of phytoplankton biomass to changes in bivalve grazing intensity (6). The mean biomass of suspension-feeding bivalves (e.g., *Corbula amurensis*, *Venerupis japonica*, *Musculista senhousia*, and *Mya arenaria*) was 7.9 g m^{-2} (ash-free dry weight) in samples collected across shallow habitats in South SFB from 1987 through 1998. However, six surveys conducted after 1998 revealed surprisingly small populations (Fig. 3*A* and SI Table 1) and complete absence of these bivalves at many sampling sites, with a mean biomass of only 0.4 g m^{-2}. The ≈20-fold bivalve decline after 1998 and its coincidence with a positive Chl-*a* trend suggests that the phytoplankton increase in SFB was a response to decreased bivalve abundance and phytoplankton consumption.

Surveys by the California Department of Fish and Game provide evidence that the bivalve population collapse was, at

Fig. 2. Monthly trends of water quality in South SFB based on USGS measurements of DIN and DRP for the years 1990–2005, and surface salinity, water temperature, Chl-*a*, and SPM for the years 1978–2005. Units are percent change y^{-1}. Darker bars indicate statistically significant trends (*P* < 0.05).

Cloern *et al.*

Fig. 3. Indices of biological community change within SFB and physical changes in the adjacent California Current. (*A*) Annual median biomass of filter-feeding bivalves across shallow habitats in South SFB; numbers above squares indicate sample number per year. (*B*) Mean annual catch ha^{-1}, normalized to 1980–2005 averages, of English sole, Bay shrimp, and Dungeness crab, from monthly sampling across the marine domains of SFB. (*C*) Anomalies in upwelling intensity computed by the National Oceanic and Atmospheric Administration from atmospheric pressure fields. (*D*) Sea surface temperature measured at the Farallon Islands. The bottom series (*C* and *D*) are 12-mo running averages of deviations from 1977–2005 monthly means.

least partly, a result of increased predation. Cumulative abundance of *Crangon* shrimp and juvenile Dungeness crab (*Cancer magister*) and English sole (*Parophrys vetulus*) increased to record levels in SFB after 1999 and persisted at high stock densities (Fig. 3*B*). These species are widespread predators in SFB that feed on benthic invertebrates including bivalve mollusks. The sum of their mean abundances (normalized to 1980–2005 means) was 7.1 from 2000 through 2004 compared with 1.8 over the preceding 20 years. Fluctuations of bivalve biomass are strongly associated with interannual and decadal changes in the abundances of their predators: bivalve recruitment has failed in other estuaries during years of high predator (*Crangon* spp.) abundance (7), and collapse of bay scallop stocks in the coastal Atlantic coincided with increased abundances of bottom-feeding skates and rays (8).

Discussion

The unexpected phytoplankton increase in SFB was one component of a broad suite of biological community changes that began after 1998 and appear to be linked through a trophic cascade (9). Abundance records suggest that heightened predation by fish and crustaceans reduced bivalve abundance and phytoplankton consumption, allowing algal biomass to grow and episodic blooms to develop after spring. Such trophic cascades have been induced through experimental additions of predatory fish in lakes (10), and large-scale community changes cascade across trophic levels in marine ecosystems when apex predators

are removed by fishing (8, 11). Trophic cascades induced by human activities can exacerbate the harmful consequences of nutrient enrichment: harvest of oysters and removal of their filtration function has contributed to the large buildup of phytoplankton biomass and associated water-quality degradation of Chesapeake Bay (12). Our observations highlight again the powerful top-down control of phytoplankton biomass by bivalve suspension feeders in shallow marine ecosystems, manifested elsewhere as abrupt phytoplankton decreases after bivalve invasions from introductions of alien species (13) or hydrologic manipulations (14).

The trophic cascade described here was not associated with changes in fishing intensity, species introductions, or other human interventions. However, it coincided with pronounced physical changes in the California Current System (CCS), suggesting that it might be linked to coupled physical and biological changes in the northeast Pacific Ocean. The 1997–1998 El Niño was the strongest on record (15), and it was followed by an equally strong La Niña in 1999. This abrupt El Niño–La Niña transition across the Pacific basin initiated a multiyear period of strong upwelling and enhanced southerly flow in the California Current that transported subarctic waters along the coast (16). At the latitude of SFB, these changes were seen as sustained positive upwelling anomalies and low surface temperature at the Farallon Islands from 1999 through 2004 (Fig. 3 *C* and *D*). Current measurements and drifter studies also documented unusually strong southward advection off Oregon, producing an equatorward displacement anomaly of 2,000 km during 2001–2002 and a source of cold water from northern latitudes (17). This "cold phase" of the East Pacific induced a suite of ecological changes along the North American coast, including southerly displacement of pelagic species and increased primary production, zooplankton biomass, and populations of cold-water pelagic fish (18).

The coincidental timing of phytoplankton increase in SFB with altered coastal currents suggests a coupling between SFB and the CCS through high annual variability in the recruitment of marine species whose juvenile stages immigrate into estuaries. This variability may occur through multiple mechanisms. Distributions of adult Dungeness crab and English sole are normally centered above the latitude of SFB, so cooling of the CCS may lead to southerly displacement of adult stocks whose distributions shift with changes in coastal temperature (19). Annual recruitment of Dungeness crab is strongest during cool years in the CCS as a result of reduced egg mortality, enhanced transport of pelagic larvae to settlement areas, or high primary production and food supply rates characteristic of La Niña-type conditions (20). The specific mechanisms of recruitment variability are unknown and likely vary among species. However, the coherent physical changes in the CCS and increased immigration of juvenile flatfish and crustaceans inside SFB are strong evidence that atmospherically driven changes in ocean boundary currents can induce large biological changes within estuaries (21). These changes can include trophic cascades leading to increased primary production and more efficient transformation of land-derived nutrients into algal biomass.

We suspect that there are subtle but important secondary manifestations of the trophic cascade outlined above. For example, the coastal Pacific is a source of phytoplankton biomass to SFB when blooms develop offshore and cells are transported into the Bay by tidal pumping (22). The new seasonal blooms after 1998 were dominated by large diatom species (e.g., *Thalassiosira punctigera*) characteristic of CCS communities during upwelling events, or dinoflagellates (e.g., *Akashiwo sanguinea*) after upwelling relaxation (4). Amplified cycles of upwelling and relaxation during cold phases of the East Pacific can provide either a significant amount of coastal-produced phytoplankton biomass (21, 23) or resting stages or vegetative cells to seed subsequent blooms within estuaries

ECOLOGY

(24). Much of the imported biomass to SFB was presumably consumed by bivalves when they were abundant (pre-1999), just as imported phytoplankton are rapidly consumed by oysters in the upwelling-influenced Willapa Bay (23). Conversely, ocean-derived phytoplankton biomass can persist or grow in SFB when bivalve abundance is low. Thus, although the steady increase in phytoplankton biomass after 1998 (Fig. 1*B*) seems to reflect growth within SFB, the new seasonal blooms (Fig. 1*A*) may be supplied at least in part by coastal phytoplankton species. Nonetheless, the appearance of these new seasonal blooms is ultimately conditional on the trophic cascade that enhances algal population growth within the SFB.

The guiding paradigm of estuarine ecology is that runoff from land is the essential driver of biological and water-quality variability. We illustrate how the coastal ocean can be an equally powerful driver of estuarine change. Oceanographers and atmospheric scientists have learned how redistributions of major atmospheric pressure systems over ocean basins can alter winds, coastal currents, water temperature, and productivity, leading to regime changes in the abundance and distribution of fish, birds, and mammals (25). Our observations in SFB began in 1977, coincidentally the last regime change of the Pacific Decadal Oscillation (PDO) (26) when the East Pacific entered a "warm phase" of weak coastal upwelling and reduced southerly transport by the California Current. Unprecedented biological changes across three trophic levels occurred in SFB after the East Pacific returned to a state approximating the cold phase of the PDO. More than two decades of observation were required to discover how an oceanic regime change can induce an altered ecological state of a large estuary.

Long-term observations of SFB reveal a previously unrecognized mode of ecosystem variability that has implications for the way we study and manage estuaries. Estuaries are the most degraded marine ecosystems (12), and recent assessments highlight the growing environmental and societal costs of this degradation (27), motivating a sense of urgency to implement strategies of ecosystem-based rehabilitation and sustainability (28). Our study suggests that programs to rehabilitate damaged estuaries should build from a broadened geographic reference that includes the interplay between processes occurring over ocean basins and within watersheds, and an expanded temporal reference that includes natural cycles and trends of ocean-atmosphere variability operating over multiple decades.

Data and Methods

Hydrography and Water Quality. We analyzed results of near-surface measurements at eight stations in South SFB where the 1978–2005 data record contains few gaps and trend tests can be applied (USGS stations 21, 22, 24, 25, 27, 29, 30, and 32; see SI Fig. 4). Chl-*a* was measured from *in vivo* fluorescence with calibration of fluorometers (Turner Designs Model 10 before 1987, and Sea Tech or Turner Designs SCUFA since 1987) using 10–20 discrete measures of extracted Chl-*a* from filtered samples each cruise (29). Daily calibrations were necessary because of significant fluctuations in the fluorescence:Chl-*a* ratio. Water samples were preserved in acid Lugol's solution and examined by light microscopy to identify, measure, and count phytoplankton cells (30).

From 1978 to 1987, salinity, temperature, and SPM concentration were measured by pumping bay water to a shipboard salinometer, thermistor, and nephelometer. Since 1987, these constituents have been measured by using a Seabird SBE 9/11 CTD and optical backscatter sensor (OBS). The nephelometer and OBS were calibrated each cruise with discrete measures of SPM determined as dry mass retained on 0.4-μm polycarbonate filters. Nutrient samples were filtered through 0.4-μm polycarbonate filters and frozen until analyzed for DIN (DIN = NH_4^+ + NO_3^- + NO_2^-) and DRP by using modifications of standard colorimetric methods (31). The light attenuation coefficient *k*

(m^{-1}) was computed from vertical irradiance profiles measured with a LI-COR 192S quantum sensor. We used a linear model to estimate *k* from SPM ($k = 0.567 + 0.0586 \times$ SPM; adjusted $R^2 = 0.863$) when light profiles were not measured. All data are available online (http://sfbay.wr.usgs.gov/access/wqdata).

Primary Production. Direct measurements of gross primary production were used to build an empirical model (SI Fig. 5) for calculating primary production over the full record of Chl-*a* and turbidity measurements. For each day and station, we first calculated the median SPM and Chl-*a* concentrations for depths ≤3 m. Under the assumptions that vertical attenuation of photosynthetically available radiation (PAR) does not change with depth, Chl-*a* is vertically homogeneous, and primary production is proportional to light absorbed by photosynthetic pigments, gross primary production (GPP) for a given location and day can be estimated from

$$GPP = \frac{4.6\Psi B I_0}{k}, \qquad \textbf{[1]}$$

where Ψ (mg C [mg Chl-*a*]$^{-1}$ [mol m^{-2}]$^{-1}$) is the water column light utilization efficiency, *B* (mg m^{-3}) is the median Chl-*a* in the upper 3 m, and I_0 [E (einstein = 1 mol of photons) m^{-2} d^{-1}] is the photosynthetically active radiation. This approach has been verified in many estuarine systems when Ψ is calibrated for local conditions. The value used here ($\Psi = 0.82$) is based on 60 ^{14}C-uptake assays conducted in SFB between 1993 and 1998 (SI Fig. 5).

The longest period of relevant solar irradiance data were provided by an annually calibrated LI-COR 192 quantum sensor mounted on the USGS R/V *Polaris* during 1980–1994. The nearest sensor covering the entire period of interest is located at Davis, California, but irradiance at the latter location averages ≈10% higher due to a lower incidence of fog. The Davis time series did allow us to verify that there was no secular trend in irradiance during the entire period. We computed GPP from an average annual cycle (SI Fig. 6) calculated from the 1980–1994 quantum sensor data and then smoothed using a spline with 30 d.f. (http://finzi.psych.upenn.edu/R/library/stats/html/smooth.spline.html).

Daily GPP estimates were linearly interpolated to provide a continuous record at each station. UTM coordinates were used to determine the straight-line distances between adjacent stations: $L_1, \ldots, L_7$. The transect-average GPP for any time period was calculated as

$$GPP_{bay} = \frac{\sum\limits_{i=1}^{7} L_i \frac{(GPP_i + GPP_{i+1})}{2}}{\sum\limits_{i=1}^{7} L_i}, \qquad \textbf{[2]}$$

where GPP_{bay} is the transect average and GPP_i is the value for station *i*. Estimates were made only for those years in which data were available for at least 75% of the month × station data matrix.

Estimation of Monthly Water Quality Trends. Long-term trends for Chl-*a*, salinity, temperature, and SPM (Fig. 2) were calculated by using USGS data collected at stations 21, 22, 24, 25, 27, 29, 30, and 32 from January 1978 through December 2005. All samples from the upper 3 m were aggregated by their median for each sampling time and location. The spatially weighted average of each water quality variable for each transect was then calculated as

$$C_{\text{bay}} = \frac{\sum_{i=1}^{7} L_i \frac{(C_i + C_{i+1})}{2}}{\sum_{i=1}^{7} L_i}, \qquad [3]$$

where C_{bay} is the transect average and C_i is the value for station i. The long-term trend for each water quality variable by month was then calculated as the Theil–Sen slope, which is the median slope of the lines joining all pairs of points in the same month but in different years. The statistical significance of the slope for each month was determined by the Mann–Kendall test (32).

Long-term trends for DIN and DRP (Fig. 2 *A* and *B*) were calculated by using data collected from January 1990 through December 2005 (earlier records are too sparse to include in trend tests). All samples within 0–3 m from the surface were aggregated by their median for each sampling time and location. Transects for each sampling day were summarized by the median value of all available data, rather than weighted averages, because of missing data. The long-term trends and their statistical significance were then calculated as above.

Estimation of Windowed Chlorophyll Trends. Windowed (decadal) trends for Chl-*a* used the same data as for the long-term monthly trends. Trends were determined for each successive decade ending in the years 1987–2005. Trends were calculated by the overall Theil–Sen slope; i.e., using lines joining all pairs of data points in the same month but in different years. The statistical significance of each trend was determined by the seasonal Kendall test, corrected for serial correlation (32). All calculations and tests, unless otherwise specified, were carried out in the R software environment (33). The *USGS Library for S-Plus* was used for the seasonal Kendall tests (34).

Bivalve Filter Feeders. Several independent research or monitoring surveys sampled benthic macrofauna across shallow habitats in the southernmost regions of South SFB from 1987 through 2005. From results of these surveys, we estimated the biomass (ash-free dry tissue weight) of filter-feeding bivalves using abundances, size distributions, and length–weight relationships determined for individual species. Sampling protocols varied

among studies, and general length–weight relationships were applied when these were not measured (SI Table 1).

Demersal Fish, Crabs, and Bay Shrimp. The California Department of Fish and Game has sampled fish, crabs, and shrimp in open-water habitats of SFB since 1980 (www.delta.dfg.ca.gov/baydelta/monitoring/baystudy.asp). Demersal species were sampled with an otter trawl having a 2.5-cm stretch mesh body and a 1.3-cm stretch mesh cod end. We present the annual mean catch per unit effort (CPUE, number ha^{-1}) from monthly (February through October) sampling at 24 stations in the marine domains of SFB (South SFB, Central SFB, and San Pablo Bay). CPUE was calculated for each species as total catch divided by area swept during a 5-min trawl at each station ($n = 5,486$). We present the mean annual CPUE, normalized to 1980–2005 means, for three benthivorous predators: juvenile English sole (*Parophrys vetulus*), juvenile Dungeness crab (*Cancer magister*), and Bay shrimp (*Crangon franciscorum*, *Crangon nigricauda*, and *Crangon nigromaculata*).

Oceanographic Data. We used the monthly Upwelling Index computed by the National Oceanic and Atmospheric Administration Pacific Fisheries Environmental Laboratory from surface atmospheric pressure fields (www.pfeg.noaa.gov/products/PFEL/modeled/indices/upwelling/NA/upwell_menu_NA.html). We report the mean of upwelling indices computed at 36°N and 39°N, stations that bound the entrance to SFB. Sea surface temperature (SST) was measured at the Farallon Islands by the Point Reyes Bird Observatory (http://shorestation.ucsd.edu/active/index_active.html). The series presented here (Fig. 3 *C* and *D*) are 12-mo running averages of monthly deviations from 1977–2005 monthly means to remove seasonal effects and highlight departures from normal patterns of upwelling and SST in the California Current.

1. Cloern JE (2001) *Mar Ecol Prog Ser* 210:223–253.
2. Nichols FH, Cloern JE, Luoma SN, Peterson DH (1986) *Science* 231:567–573.
3. Cloern JE (1996) *Rev Geophys* 34:127–168.
4. Cloern JE, Schraga TS, Lopez CB, Knowles N, Labiosa RG, Dugdale R (2005) *Geophys Res Lett* 32:LI4608.
5. Smith SV, Hollibaugh JT (2006) *Limnol Oceanogr* 51:504–517.
6. Lucas LV, Koseff JR, Cloern JE, Monismith SG, Thompson JK (1999) *Mar Ecol Prog Ser* 187:1–15.
7. Beukema JJ, Dekker R (2005) *Mar Ecol Prog Ser* 287:149–167.
8. Myers RA, Baum JK, Shepherd TD, Powers SP, Peterson CH (2007) *Science* 315:1846–1850.
9. Pace ML, Cole JJ, Carpenter SR, Kitchell JF (1999) *TREE* 14:483–488.
10. Carpenter SR, Cole JJ, Hodgson JR, Kitchell JF, Pace ML, Bade D, Cottingham KL, Essington TE, Houser JN, Schindler DE (2001) *Ecol Monogr* 71:163–186.
11. Daskalov GM, Grishin AN, Rodionov S, Mihneva V (2007) *Proc Natl Acad Sci USA* 104:10518–10523.
12. Jackson JBC, Kirby MX, Berger WH, Bjorndal KA, Botsford LW, Bourque BJ, Bradbury RH, Cooke R, Erlandson J, Estes JA, *et al.* (2001) *Science* 293:629–638.
13. Alpine AE, Cloern JE (1992) *Limnol Oceanogr* 37:946–955.
14. Petersen JK, Hansen JW, Laursen MB, Clausen P, Carstensen J, Conley DJ, *Ecol Appl*, in press.
15. McPhaden MJ (1999) *Science* 283:950–954.
16. Freeland HJ, Gatien G, Huyer A, Smith RL (2003) *Geophys Res Lett* 30:1141.
17. Kosro PM (2003) *Geophys Res Lett* 30:8023.
18. Peterson WT, Schwing FB (2003) *Geophys Res Lett* 30:1896.

19. Perry AL, Low PJ, Ellis JR, Reynolds JD (2005) *Science* 308:1912–1915.
20. Botsford LW, Lawrence CA (2002) *Prog Oceanogr* 53:283–305.
21. Roegner GC, Shanks AL (2001) *Estuaries* 24:244–256.
22. Martin MA, Fram JP, Stacey MT (2007) *Mar Ecol Prog Ser* 337:51–61.
23. Banas NS, Hickey BM, Newton JA, Ruesink JL (2007) *Mar Ecol Prog Ser* 341:123–139.
24. Smayda TJ (2002) *Harmful Algae* 1:95–112.
25. McGowan JA, Cayan DR, Dorman LM (1998) *Science* 281:210–217.
26. Mantua NJ, Hare SR, Zhang Y, Wallace JM, Francis RC (1997) *Bull Am Meteorol Soc* 78:1069–1079.
27. Worm B, Barbier EB, Beaumont N, Duffy JE, Folke C, Halpern BS, Jackson JBC, Lotze HK, Micheli F, Palumbi SR, *et al.* (2006) *Science* 314:787–790.
28. Lotze HK, Lenihan HS, Bourque BJ, Bradbury RH, Cooke RG, Kay MC, Kidwell SM, Kirby MX, Peterson CH, Jackson JBC (2006) *Science* 312:1806–1809.
29. Cloern JE (1991) *J Mar Res* 49:203–221.
30. Cloern JE, Dufford R (2005) *Mar Ecol Prog Ser* 285:11–28.
31. Hager SW, Schemel LE (1997) *Dissolved Nutrient Data for the San Francisco Bay Estuary California, January Through November 1995* (US Geological Survey, Menlo Park, CA), US Geological Survey Open-File Report 97-359.
32. Helsel DR, Hirsch RM (1992) *Statistical Methods in Water Resources* (Elsevier, New York).
33. R Development Core Team (2005) *R: A Language and Environment for Statistical Computing* (R Foundation for Statistical Computing, Vienna).
34. Slack JR, Lorenz DL, *et al.* (2003) *USGS Library for S-PLUS for Windows*, Release 2.1, US Geological Survey Open-File Report 03-357.

ECOLOGY